*Available online www.jsaer.com*

***Journal of Scientific and Engineering Research*, 2017, 4(1):13-21**


**Research Article**

**ISSN: 2394-2630**
**CODEN(USA): JSERBR**

# A systematic, theoretical study of non-carrier added $^{64}$Cu production with low energy medical cyclotrons

**Lucrezia Auditore[1]*, Ernesto Amato[2,3], Sergio Baldari[1,2]**

[1]Nuclear Medicine Unit, University Hospital "G. Martino", Messina, Italy
[2]Section of Radiological Sciences, Department of Biomedical and Dental Sciences and GruppoCollegato di Messina, IstitutoNazionale di FisicaNucleare, Messina, Italy
[3]Morphofunctional Imaging, University of Messina, Messina, Italy

**Abstract** $^{64}$Cu isotope finds increasing theranostic applications in PET and nuclear medicine therapies. Clinically relevant $^{64}$Cu activities can be produced by proton irradiation of enriched metal targets.

This work presents a systematic theoretical study of non-carrier added$^{64}$Cu production pathways with Ni and Zn enriched targets bombarded by protons accelerated by a low-energy medical cyclotron, evaluating the contribution of all the competing channels when degrading proton energy, changing target thickness and irradiation or cooling times, with the aim of optimizing such parameters and providing an overview of $^{64}$Cu production.

$^{64}$Cu production from 95% $^{64}$Ni and 97% $^{67}$Zn enriched targets were considered. Yields at the End Of Bombardment (EOB) were calculated through TALYS code and an analytical computation based on the EXFOR experimental data libraries and on Bragg curves in targets evaluated with MCNPX Monte Carlo code. A validation of our theoretical estimations was obtained through a comparison with experimental data, when available in literature.

The comparison between the two investigated pathways allows to point out the potential advantages of each method to be selected basing on the specific needs of production.

**Keywords** Copper-64; positron emission tomography; cyclotron; TALYS; EXFOR

## 1. Introduction

The $^{64}$Cu isotope, with an half-life of 12.64 hs and a multiple decay mode ($\beta^-$, $\beta^+$, E.C.), is a promising theranostic nuclide for PET and nuclear medicine treatments of cancer [1-4]. Nowadays, clinically relevant non-carrier added $^{64}$Cu activities can be obtained by the nuclear reaction $^{64}$Ni(p,n) $^{64}$Cu on (95%-99%) $^{64}$Ni enriched targets [5-12] and alternative production pathways are being studied [13-18]. After irradiation, the target contains $^{64}$Cu mixed with other isotopes. Properly choosing beam parameters, target composition, thickness and shape, irradiation and cooling times, it is possible to achieve a valuable reduction of contaminants.

This work aims to provide a systematic study of the non-carrier added $^{64}$Cu production with Ni and Zn enriched targets, evaluating the contribution of all the competing channels and can help to improve quality and overall production yield when setting up a cyclotron plant for copper-64 production.

## 2. Materials and methods

$^{64}$Cu production with proton-induced reactions can follow different pathways. In this paper $^{64}$Cu production exploiting enriched $^{64}$Ni and $^{67}$Zn targets were analysed. Table 1 lists the assumed isotopic compositions of both

targets together with the all the possible reaction channels open at 11 MeV contributing to the formation of unwanted contaminant nuclides.

**Table 1:** Target compositions, reactions and produced nuclides.

| Target isotope | Abund. (%) | Reaction | $E_{th}$ (MeV) | Product | $t_{1/2}$ |
|---|---|---|---|---|---|
| | | Enriched Ni target | | | |
| $^{64}$Ni | 95.0 | (p,n), (p,γ), (p,α) | 2.66, 0.0, 0.0 | $^{64}$Cu, $^{65}$Cu, $^{61}$Co | 12.64 h, stable, 1.65 h |
| $^{58}$Ni | 3.416 | (p,α) | 1.36 | $^{55}$Co | 17.53 h |
| $^{60}$Ni | 1.3225 | (p,n), (p,γ), (p,α) | 7.09, 0.0, 0.27 | $^{60}$Cu, $^{61}$Cu, $^{57}$Co | 23.67 m, 271.74 d |
| $^{61}$Ni | 0.0685 | (p,n), (p,γ), (p,α) | 3.55, 0.0, 0.0 | $^{61}$Cu, $^{62}$Cu, $^{58}$Co | 3.33 h, 9.67 m, 70.86 d |
| $^{62}$Ni | 0.193 | (p,n) | 4.86 | $^{62}$Cu | 9.67 m |
| | | Enriched Zn target | | | |
| $^{67}$Zn | 97.0 | (p,n),(p,γ), (p,α) | 1.98, 0.0, 0.0 | $^{67}$Ga, $^{68}$Ga, $^{64}$Cu | 3.26 d, 1.13 h, 12.64 h |
| $^{64}$Zn | 1.537 | (p,n), (p,γ), (p,α) | 8.12, 0.0, 0.0 | $^{64}$Ga, $^{65}$Ga, $^{61}$Cu | 2.63 m, 15.2 m, 3.33 h |
| $^{66}$Zn | 0.867 | (p,n), (p,γ) | 6.09, 0.0 | $^{66}$Ga, $^{67}$Ga | 9.5 h, 3.26 d |
| $^{68}$Zn | 0.577 | (p,n), (p,γ), (p,α) | 3.94, 0.0, 0.0 | $^{68}$Ga, $^{69}$Ga,$^{65}$Cu | 1.13 h, stable, stable |
| $^{70}$Zn | 0.019 | (p,n), (p,α) | 1.97, 0.0 | $^{70}$Ga, $^{67}$Cu | 21.13 m, 2.58 d |

Yields at the End Of Bombardment (EOB) were estimated using two approaches.

Firstly, the TALYS v.1.8 nuclear reaction code [19] as employed in the *medical isotope production* modality that allows computing the production yields in homogenous, thick targets for all the reaction channels energetically allowed. In particular, since a single target isotope can be assigned, calculations were carried out for each constituent isotope and then weighted for the relative abundance. TALYS implements nuclear reaction models to compute excitation functions that build up the TALYS-based Evaluated Nuclear Data Library (TENDL) cross section data libraries [20].

Furthermore, an analytical approach based on experimental data picked from the EXFOR database [21] making use of the Bragg curve in the target estimated with Monte Carlo N Particle eXtended (MCNPX) code [22] was implemented.

$Yields_{EOB}$ were estimated following the approach described in IAEA Technical Report No. 468 [23]:

$$Y_{EOB} = \frac{N_A I}{A_T}\left(1 - e^{-\lambda t}\right)\int_{E_{th}}^{E_{beam}} \sigma_T(E)\frac{dE}{S_T(E)} \quad (1)$$

where$N_A$ is Avogadro's number; $I$, the proton beam current; $A_T$, the atomic weight of the target material; $\lambda$, the decay constant of the produced isotope; $E_{th}$, the threshold energy for the reaction channel; $E_{beam}$, the proton beam energy; $\sigma_T(E)$, the total cross section for the considered reaction channel; $S_T(E)$, the stopping power.

$S_T(E)$ was computed carrying out a MCNPX simulations considering Ni and Zn targets according to the chosen enrichment. $\sigma_T(E)$ was obtained fitting the EXFOR experimental cross section data for the considered channels.

To validate the analytical method, $\sigma_T(E)$ was also estimated by fitting TENDL-2015 cross section data. The evaluated nuclide yields were then compared with the ones provided by TALYS which in turn uses the same nuclear reaction models on which TENDL libraries are based. Theoretical results were also compared with experimental data when available in literature [7,10].

Nuclide yields were estimated as a function of depth in target, proton beam energy, irradiation and cooling time. Discussed results as a function of depth in target and proton energy are referred to 1 h EOB.

## 3. Results

*Nickel target*

The analytical approach was validated by comparing the radionuclide production yields estimated using TENDL cross section libraries with those predicted by TALYS. Table 2 reports the results of this comparison, carried out for 11 MeV protons irradiating Ni target for 1 h.

**Table 2:**Validation of the analytical method

| | TALYS | | MCNPX-TENDL2015 | |
|---|---|---|---|---|
| | **Yield [MBq/μA]** | **Relative yield to $^{64}$Cu** | **Yield [MBq/μA]** | **Relative yield to $^{64}$Cu** |
| $^{64}$Cu | 3.74E+02 | 1.00E+00 | 3.97E+02 | 1.00E+00 |
| $^{61}$Co | 9.90E+00 | 2.65E-02 | 1.10E+01 | 2.77E-02 |
| $^{55}$Co | 5.01E-02 | 1.34E-04 | 6.18E-02 | 1.56E-04 |
| $^{60}$Cu | 2.14E+01 | 5.72E-02 | 2.41E+01 | 6.06E-02 |
| $^{57}$Co | 1.66E-04 | 4.43E-07 | 1.97E-04 | 4.97E-07 |
| $^{58}$Co | 8.99E-05 | 2.40E-07 | 1.54E-04 | 3.89E-07 |
| $^{61}$Cu | 5.43E-01 | 1.45E-03 | 5.70E-01 | 1.44E-03 |
| $^{62}$Cu | 1.08E+01 | 2.89E-02 | 1.18E+01 | 2.98E-02 |

Fig. 1 shows the comparison between the radionuclide production yields as a function of depth in the target, as expected from both calculation methods when irradiating for 1 h with 11 MeV protons a thick target of enriched $^{64}$Ni composed as in Table 1.

It can be seen that $^{64}$Cu is produced together with $^{60,61,62}$Cu and $^{55,57,58,61}$Co nuclides.

The most important contaminant produced nuclides are $^{60}$Cu, $^{62}$Cu and $^{61}$Co, whose yields are about 1.5 order of magnitude lower than $^{64}$Cu. Yields 3-4 order of magnitudes lower than $^{64}$Cu are predictable for $^{61}$Cu and $^{55}$Co, respectively, while the lowest yields are expected for $^{57,58}$Co.

The production profile as a function of depth in target is determined by the energy dependence of reaction cross sections. The high reaction energy threshold for $^{60}$Cu causes the abrupt cut-off of its production around 150 μm of depth in target, while $^{61,62}$Cu production after 210 μm is sustained by (p,γ) reaction channel.

The agreement between EXFOR-based and TALYS results is good for higher energies (low depths) but some differences exists for lower energies. These differences can be partially addressed to the availability of experimental data in the EXFOR database, partially to the inherent differences between the experimental data and the theoretical models TALYS relies on.

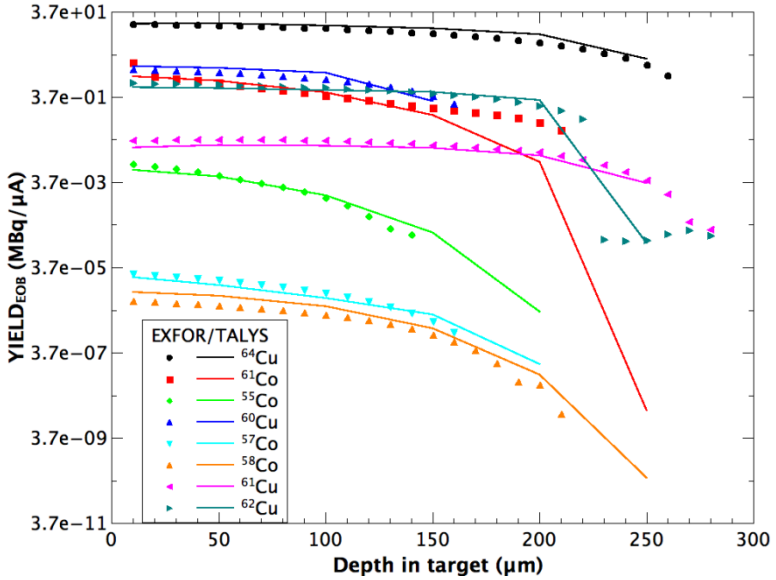


*Figure 1: Radionuclide yields after 1 h of proton irradiation evaluated as a function of depth inside an enriched $^{64}$Ni thick target; comparison between EXFOR-based and TALYS estimations.*

Fig. 2 shows how the incident proton energy can influence the production yields. One-hour irradiation is still adopted. Lowering proton energy (e.g. by means of an aluminium degrader or changing particle accelerating parameters) changes the ratios between $^{64}$Cu and the unwanted nuclides. In particular, it is possible to choose an 'optimal' proton beam energy in order to reduce, or even forbid, the production of contaminant nuclides. Reducing proton energy to 5 MeV, $^{64}$Cu yieldslowers to 34.04MBq/μA, while $^{60}$Cuand $^{55,57,58}$Co are not

produced or detectable any more, $^{61}$Cu and $^{61}$Co lowers to less than 3.7E-02MBq/μA, $^{62}$Cu lowers to about 3.7E-01MBq/μA.

Same considerations hold as above about the comparison between EXFOR-based and TALYS results.

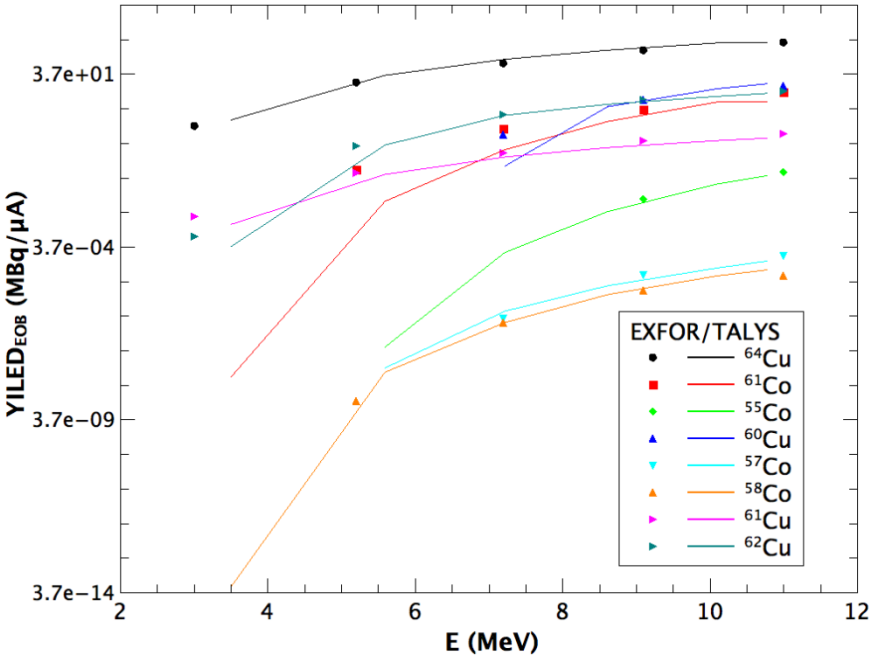


*Figure 2: Radionuclide yields after 1 h of proton irradiation on an enriched $^{64}$Ni thick target, evaluated as a function of incident proton energy; comparison between EXFOR-based and TALYS estimations*

In Fig. 3, the yields as a function of time are shown for 11 MeV proton irradiation. A reasonable 3 h irradiation is adopted to show the influence of half-life on the production and decay rates of $^{64}$Cu and contaminant nuclides. $^{60,62}$Cu rapidly saturate due to their short half-lives thus improving $^{64}$Cu to $^{60,62}$Cu production ratios.

For the same reason the presence of these contaminants can be significantly reduced by choosing the proper cooling time.

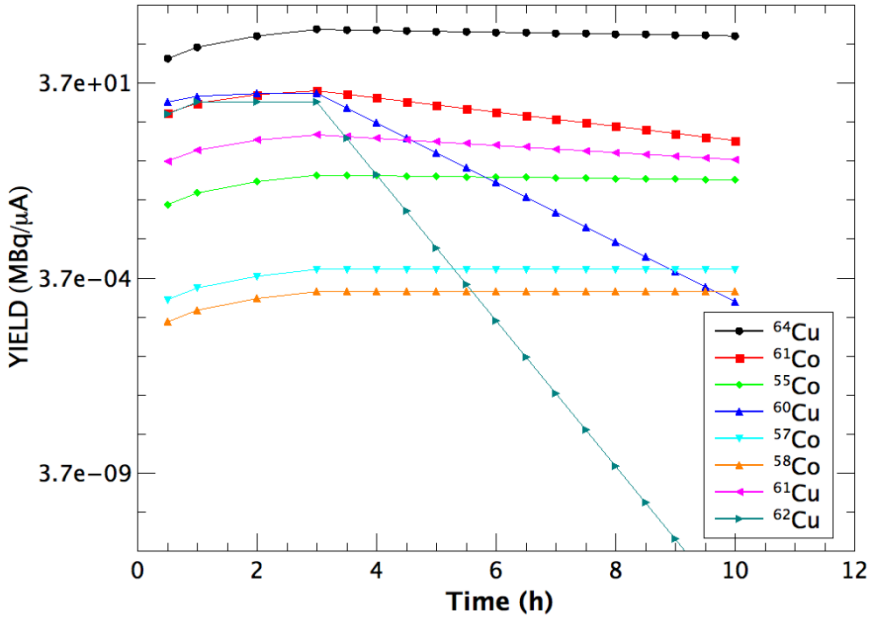


*Figure 3: Radionuclide yields after 3 hs of proton irradiation on an enriched $^{64}$Ni thick target, evaluated as a function of time.*

Table 3 shows a comparison between the obtained theoretical results and the experimental data measured byAvila-Rodriguez et al. [10] and Jeffery et al. [7]. The data reported show a qualitative agreement between production yields and differences can be attributed to minor differences in proton energy, target thickness and actual $^{64}$Ni enrichment (96% [10] and 94.8% [7]).

**Table 3:** Yield of nuclides in an enriched $^{64}$Ni thick target irradiated with 11 MeV protons for 1 h. Comparison between theoretical estimations and experimental data available in literature.

| | $E_p$=11 MeV | | | | $E_p$=11.4 MeV | $E_p$=11.7 MeV |
|---|---|---|---|---|---|---|
| | TALYS | | EXFOR | | Avila-Rodriquez [10] | Jeffery [7] |
| | Yield | Relative yield | Yield | Relative yield | Relative yield | Relative yield |
| **$^{64}$Cu** | 3.74E+02 | 1.00E+00 | 3.05E+02 | 1.00E+00 | 1.00E+00 | 1.00E+00 |
| **$^{61}$Co** | 9.90E+00 | 2.65E-02 | 1.12E+01 | 3.66E-02 | ND | 1.61E-02 |
| **$^{55}$Co** | 5.01E-02 | 1.34E-04 | 6.12E-02 | 2.01E-04 | ND | 6.56E-04 |
| **$^{60}$Cu** | 2.14E+01 | 5.72E-02 | 1.79E+01 | 5.88E-02 | 6.21E-02 | 9.59E-02 |
| **$^{57}$Co** | 1.66E-04 | 4.43E-07 | 2.18E-04 | 7.14E-07 | - | ND |
| **$^{58}$Co** | 8.99E-05 | 2.40E-07 | 5.74E-05 | 1.88E-07 | - | - |
| **$^{61}$Cu** | 5.43E-01 | 1.45E-03 | 7.30E-01 | 2.40E-03 | 3.20E-03 | 2.79E-03 |
| **$^{62}$Cu** | 1.08E+01 | 2.89E-02 | 1.22E+01 | 4.01E-02 | 6.27E-02 | ND |

*Zinc target*

Fig. 4 shows the expected production yields after 1 h of irradiation at 11 MeV of a thick, enriched $^{67}$Zn target, whose composition is listed in Table 1. On such a target, $^{64}$Cu yield is overwhelmed by $^{64,67,68}$Ga isotopes while $^{65,66,70}$Ga and $^{61,67}$Cu are produced in minor quantities.

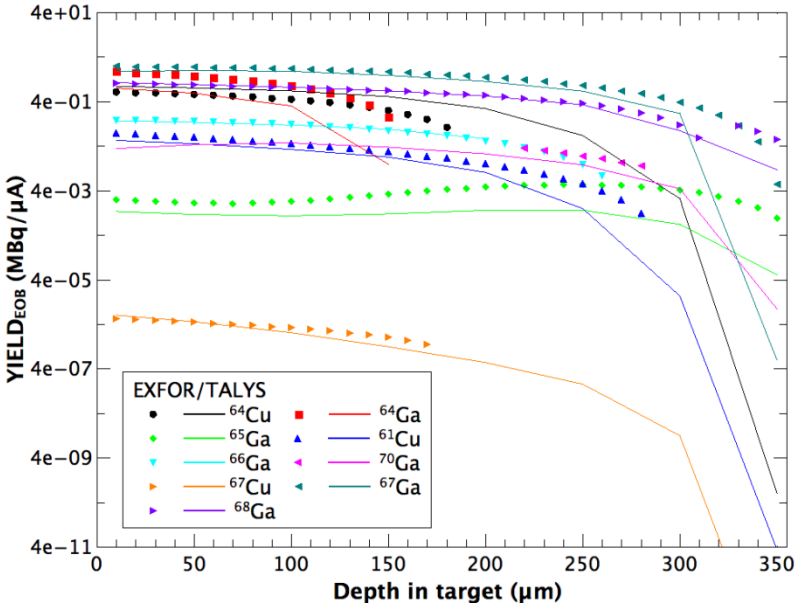


*Figure 4: Radionuclide yields after 1 h of proton irradiation evaluated as a function of depth inside an enriched $^{67}$Zn thick target; comparison between EXFOR-based and TALYS estimations*

Differently from the enriched $^{64}$Ni target case, more relevant differences between EXFOR-based and TALYS estimations are found, especially for which concerns $^{61,64}$Cu and $^{64,65}$Ga. For some proton-induced reactions on zinc target, experimental data are sparsely available in the considered energy range. As a consequence, for these production channels, the analytical approach based on EXFOR data base could estimate the yields for a limited thickness range only. Moreover, noticeable differences can be found between TENDL2015 and EXFOR cross sections.

In particular, for $^{64}$Cu only few experimental data are available in the range 7.9-11 MeV and TENDL-2015 systematically overestimates cross sections of about 10 mbarn. Particularly relevant are the differences between the EXFOR and TENDL-2015 cross sections for $^{64}$Ga and $^{65}$Ga isotopes, as reported in Fig. 5. These differences cause the underestimation of the respective yields when calculated with TALYS.

According to the results shown in Fig. 4, it can be argued that the relative yield of $^{64}$Cu with respect to the other nuclides can be maximized using a target thickness up to 100 μm.

For a 100-μm target, relative yields of $^{67,68}$Ga with respect to $^{64}$Cu are expected to be about 4.2 and 1.6, respectively, while for a 350-μm thick target these relative yields are expected to rise up to about 6.5 and 2.5, respectively.

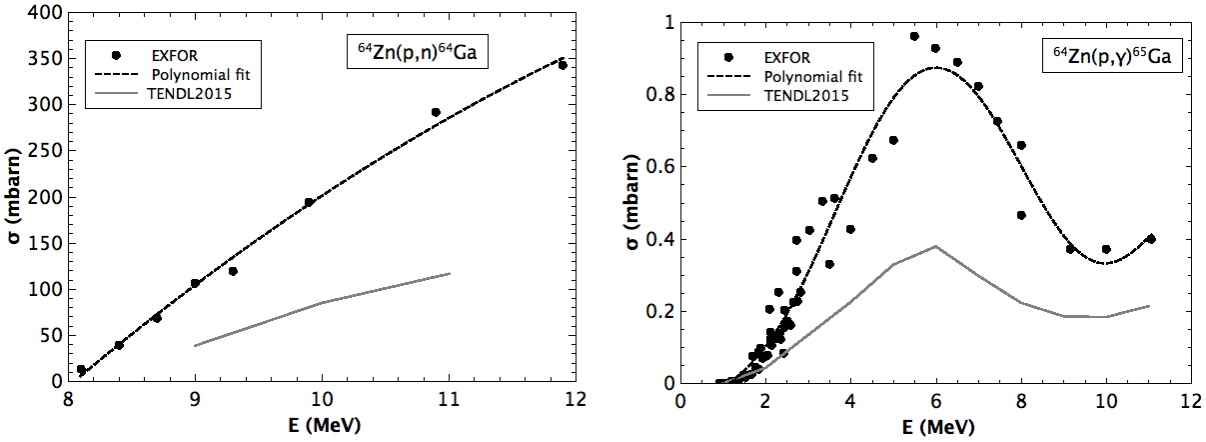


*Figure 5: Comparison between EXFOR and TALYS cross sections for $^{64}$Ga (left) and $^{65}$Ga (right) production reaction channels. Red curve is the fit used for the EXFOR-based analytical approach.*

Taking into account the threshold energy for the reactions $^{64}$Zn(p,n)$^{64}$Ga ($E_{th}$=8.12 MeV) and $^{66}$Zn(p,n)$^{66}$Ga ($E_{th}$=6.09 MeV), lowering of proton energy to 6-7 MeV reduces $^{64}$Cu yield of one order of magnitude, while $^{64}$Ga is not produced any more and $^{66}$Ga is markedly reduced, as shown in Fig. 6. However, eliminating these two gallium isotopes does not provide any advantage during the chemical process of $^{64}$Cu extraction, since $^{67}$Ga and $^{68}$Ga nuclides are still present as the most important contaminants. Moreover, the very short half-life of $^{64}$Ga ($t_{1/2}$=2.63 m) allows to drastically reduce it setting up the irradiation time to 3 h and a cooling time greater than 1 h, as shown in Fig. 7. Same considerations hold for $^{65,70}$Ga isotopes.

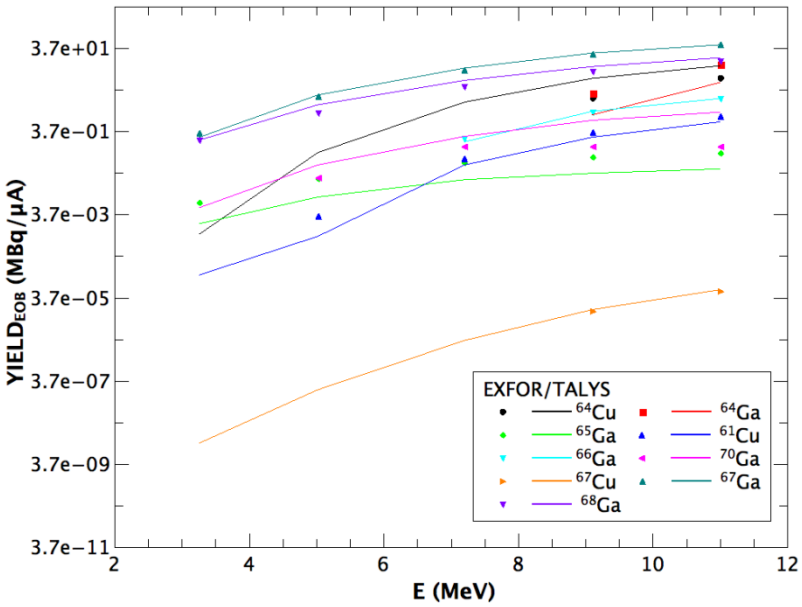


*Figure 6: Radionuclide yields after 1 h of proton irradiation on an enriched $^{67}$Zn thick target, evaluated as a function of incident proton energy; comparison between EXFOR-based and TALYS estimations*

From the chemical point of view, the worst contaminant nuclide is $^{61}$Cu whose yield is one order of magnitude lower than that of $^{64}$Cu. Moreover, its long decay time does not allow to choose an useful cooling time to remarkably reduce it (Fig. 7). As a result, a target containing both $^{64}$Cu and $^{61}$Cu is produced with a yield of a $^{61}$Cu relative to $^{64}$Cu of about 0.0487 (according to TALYS), or 0.129 (according to EXFOR-based estimation).

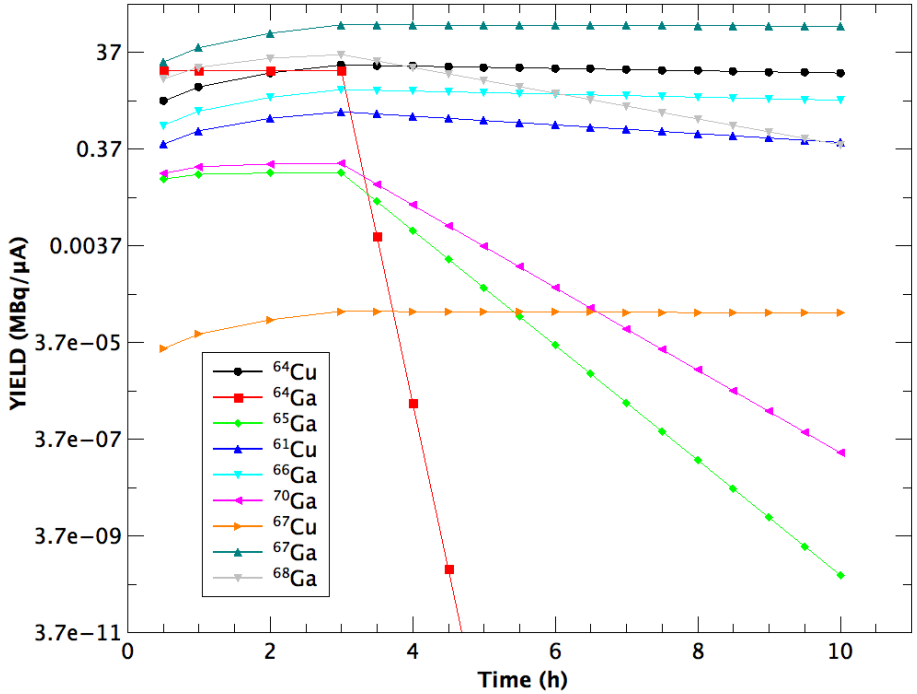


*Figure 7: Radionuclide yields after 3 hs of proton irradiation on an enriched $^{67}$Zn thick target, evaluated as a function of time*

Table 4 shows a comparison between the obtained theoretical results. As noticed above, yields of $^{64}$Cu and $^{64,65,70}$Ga as estimated by TALYS and EXFOR-based analytical method show a poor agreement. A more complete set of experimental data would be necessary to make a more confident comparison.

**Table 4:** Yield of nuclides in an enriched $^{67}$Zn thick target irradiated with 11 MeV protons for 1 h.

| | TALYS | | EXFOR | |
|---|---|---|---|---|
| | **Yield [MBq/μA]** | **Relative yield to $^{64}$Cu** | **Yield [MBq/μA]** | **Relative yield to $^{64}$Cu** |
| **$^{64}$Cu** | 1.41E+01 | 1.00E+00 | 7.14E+00 | 1.00E+00 |
| **$^{64}$Ga** | 6.14E+00 | 4.34E-01 | 1.62E+01 | 2.27E+00 |
| **$^{65}$Ga** | 4.75E-02 | 3.36E-03 | 1.16E-01 | 1.63E-02 |
| **$^{61}$Cu** | 6.88E-01 | 4.87E-02 | 9.24E-01 | 1.29E-01 |
| **$^{66}$Ga** | 2.42E+00 | 1.71E-01 | 2.29E+00 | 3.20E-01 |
| **$^{70}$Ga** | 1.04E+00 | 7.36E-02 | 1.52E-01 | 2.13E-02 |
| **$^{67}$Cu** | 5.84E-05 | 4.13E-06 | 5.24E-05 | 7.33E-06 |
| **$^{67}$Ga** | 5.81E+01 | 4.11E+00 | 4.62E+01 | 6.48E+00 |
| **$^{68}$Ga** | 2.14E+01 | 1.51E+00 | 1.79E+01 | 2.51E+00 |

## 4. Discussion

In the $^{64}$Ni enriched target case, the optimization of the process can be achieved irradiating a thick target (up to 300 μm) with 5 MeV protons; in this configuration $^{64}$Cu yields of about 34.04MBq/μA are expected and the final target includes only $^{61}$Cu, $^{61}$Co (whose yields are less than 3.7E-02MBq/μA) and $^{62}$Cu (whose yield is about 3.7E-01 MBq/μA) for 1 h EBO as contaminants.

In the $^{67}$Zn enriched target case, $^{64}$Cu is not the most abundant product and an energy cut does not provide any remarkable advantage. The degradation of proton energy to 8 MeV allows inhibiting production of $^{64}$Ga, while $^{64}$Cu yield is still reasonable. Nevertheless, the very short half-life of $^{64}$Ga ($t_{1/2}$=2.63 m) allows achieving a slightly better result by properly setting up the cooling time after irradiation.

In order to improve the yield$_{EOB}$ of $^{64}$Cu with respect to the most abundant unwanted products ($^{67,68}$Ga), targets with thickness up to 100 μm should be used. Beyond this thickness, $^{64}$Cu production decreases while the production of $^{67,68}$Ga still remains important.

As concerns $^{68}$Ga ($t_{1/2}$=1.13 h), a proper cooling time (about 7 hs) can be chosen to reduce it. Finally, the irradiated target contains also $^{61}$Cu and $^{66}$Ga as relevant contaminants.

As indicated by the results, $^{64}$Ni(p,n)$^{64}$Cu reaction is to be preferred to $^{67}$Zn(p,α)$^{64}$Cu for $^{64}$Cu production purposes. Optimizing all the parameters for the two considered pathways ($^{64}$Ni target: $E_p$=5 MeV and thickness=300 μm; $^{67}$Zn target: $E_p$=11 MeV and thickness=100 μm), at EOB 3 h, yields of $^{64}$Cu are expected to be about 34.04 MBq/μA and 2.22MBq/μA for $^{64}$Ni and $^{67}$Zn enriched target, respectively. In the first case, $^{62}$Cu is the most relevant contaminant along with $^{61}$Co and $^{61}$Cu as minor ones; in the second case, $^{67,68}$Ga are the most important produced isotopes together with $^{64}$Cu, while $^{61}$Cu and $^{66}$Ga are present in relevant quantities. Moreover, the $^{64}$Zn(n,g)$^{65}$Zn induced by secondary neutrons produced by the main reaction $^{64}$Zn(p,n)$^{64}$Ga should be also taken into account. $^{65}$Zn is a long-lived radionuclide ($t_{1/2}$=243.66 d) and although it can be chemically separated from $^{64}$Cu, can represent a problem for target recovering and radioprotection problematics.

Nevertheless, this study indicates that if $^{64}$Cu and gallium isotopes are used in the same clinical centre, proton irradiation of enriched $^{67}$Zn targets can be a route to simultaneously produce quantities of clinical interest of the two radioisotopes.

## 5. Conclusion

Clinical interest to $^{64}$Cu isotope is well established and experimental data on non-carrier added $^{64}$Cu yields are available. In this paper we provided a comprehensive theoretical analysis of two production pathways of this isotope with low energy proton beams, carrying out an overview of the parameters influencing both production yields and contamination by unwanted isotopes.

This study confirmed that, for low energy proton beams, the channel $^{64}$Ni(p,n)$^{64}$Cu is to prefer to $^{67}$Zn(p,α)$^{64}$Cu, although the second reaction can be a good solution to simultaneously produce $^{64}$Cu and $^{67,68}$Ga isotopes and can become competing for proton energies greater than 15 MeV[24].

## References


[1]. NiccoliAsabella A. et al., The copper radioisotopes: A systematic review with special interest to 64Cu. BioMed Res Internat. (2014) art. no. 786463.

[2]. Srivastava S.C., Paving the way to personalized medicine: production of some promising theragnostic radionuclides at Brookhaven national laboratory. SeminNucl Med. 42(3) (2012) 151–163.

[3]. Ferreira C.L. et al., Comparison of bifunctional chelates for $^{64}$Cu antibody imaging. Eur J Nucl Med Mol Imaging 37(11) (2010) 2117–2126.

[4]. Monica S. and Anderson C.J., Molecular imaging of cancer with copper-64 radiopharmaceuticals and positron emission tomography (PET). Accounts Chem Res. 42 (2009) 832–841.

[5]. IAEA Radioisotopes and Radiopharmaceuticals Series No. 1, Cyclotron Produced Radionuclides: Emerging Positron Emitters for Medical Applications: $^{64}$Cu and $^{124}$I. STI/PUB/1717, Vienna 2016.

[6]. Al Rayyes A.H. and Ailouti Y., Production and quality control of $^{64}$Cu from high current Ni target.World J NuclSciTechnol 3 (2013) 72-77.

[7]. Jeffery C.M. et al., Routine production of copper-64 using 11.7 MeV protons. AIP ConfProc 1509 (2012) 84-90.

[8]. Ometakova J. et al., Automated production of 64Cu prepared by 18 MeV cyclotron. J RadioanalNuclChem 293 (2012) 217-222.

[9]. Matarrese M. et al., Automated production of copper radioisotopes and preparation of high specific activity [64Cu]Cu-ATSM for PET studies. ApplRadiat Isotopes 68(1) (2010) 5-13.

[10]. Avila-Rodriguez M.A. et al., Simultaneous production of high specific activity $^{64}$Cu and $^{61}$Co with 11.4 MeV protons on enriched $^{64}$Ni nuclei. ApplRadiat Isotopes 65(10) (2007) 1115-1120.
[11]. Obata A. et al., Production of therapeutic quantities of $^{64}$Cu using a 12 MeV cyclotron. Nucl Med Biol. 30 (2003) 535-539.
[12]. McCarthy Deborah W. et al., Efficient production of high specific activity 64Cu using a biomedical cyclotron. Nucl Med Biol 24(1) (1997) 35-43.
[13]. Amato E. et al., Future laser-accelerated proton beams at ELI-Beamlines as potential source of positron emitters for PET. J Instrum 11(4) (2016) C04007.
[14]. Amato E. et al., Study of the production yields of $^{18}$F, $^{11}$C, $^{13}$N, $^{15}$O positron emitters from plasma-laser proton source at ELI-beamlines for labelling of PET radiopharmaceuticals NuclInstr Meth A 811 (2016) 1-5.
[15]. Italiano A. et al., Production of $^{68}$Ge, $^{64}$Cu, $^{86}$Y, $^{89}$Zr, $^{73}$Se, $^{77}$Br and $^{124}$I positron emitting radionuclides through future laser-accelerated proton beams at ELI-beamlines for innovative PET diagnostics. AttiAccademiaPeloritanadeiPericolanti – Classe di ScienzeFisicheMatematiche e Naturali 93 (2015) Art. no. 93.
[16]. Tadahiro K. et al., New Production Routes for MedicalIsotopes$^{64}$Cu and $^{67}$Cu Using Accelerator Neutrons. J PhysSocJpn 82 (2013) 034201.
[17]. Kozempel J. et al., A novel method for n.c.a. 64Cu production by the 64Zn(d,2p)64Cu reaction and dual ion-exchange column chromatography. Radiochem. Acta 95 (2007) 75-80.
[18]. Abbas K. et al., Cyclotron production of 64Cu by deuteron irradiation of 64Zn. ApplRadiat Isotopes 64(9) (2006) 1001-1005.
[19]. Koning A.J. et al., TALYS: Comprehensive nuclear reaction modeling. AIP ConfProc 769 (2005) 1154-1159.
[20]. Koning A.J. and Rochman D., Modern Nuclear Data Evaluation with the TALYS Code System. Nucl Data Sheets 113(12) (2012) 2927-2934.
[21]. Experimental Nuclear Reaction Data (EXFOR). Available online at: https://www-nds.iaea.org/exfor/exfor.htm
[22]. Pelowitz DB, ed., MCNPX User's Manual, Version 2.5.0, Los Alamos National Laboratory report LA-CP-05-0369 (April 2005).
[23]. IAEA Technical Report Series No. 468, Cyclotron Produced Radionuclides: Physical Characteristics and Productions Methods, Vienna 2009.
[24]. Aslam M.N. et al., Evaluation of excitation functions of the $^{68,67,66}$Zn(p,xn)$^{68,67,66}$Ga and $^{67}$Zn(p,α)$^{64}$Cu reactions: Validation of evaluated data through comparison with experimental excitation functions of the $^{nat}$Zn(p,x)$^{66,67}$Ga and $^{nat}$Zn(p,x)$^{64}$Cu processes. ApplRadiat Isotopes 96 (2015) 102-113.